Antiviral Research 163 (2019) 11–18

Contents lists available at ScienceDirect

Antiviral Research

journal homepage: www.elsevier.com/locate/antiviral

Research paper

Characterization of the molecular events of covalently closed circular DNA synthesis in *de novo* Hepatitis B virus infection of human hepatoma cells

Mehrangiz Dezhbord[a], Sooyoung Lee[b], Woohyun Kim[b], Baik Lin Seong[a,**], Wang-Shick Ryu[b,*]

[a] Department of Biotechnology, College of Life Science & Biotechnology, Yonsei University, Seoul, South Korea
[b] Department of Biochemistry, College of Life Science & Biotechnology, Yonsei University, Seoul, South Korea

ARTICLE INFO

Keywords:
HepG2-NTCP cell line
Hepatitis B infection
Time point HBV infection
cccDNA dynamics

ABSTRACT

Despite the utmost importance of cccDNA in HBV biology, the mechanism by which cccDNA synthesis is regulated is not completely understood. Here we explored HepG2-NTCP cell line and performed a time-course HBV infection experiment (up to 30 days) to follow the conversion of the input viral DNA into cccDNA. We found that a protein-free RC DNA (PF-RC DNA) become detectable as early as 12 h post infection (hpi) prior to the detection of cccDNA, which become evident only at 2–3 dpi. Intriguingly, the PF-RC DNA detected at 12 hpi was abundantly located in the cytoplasm, implicating that the protein-removal from the input viral DNA takes place in the cytoplasm, perhaps inside the nucleocapsid. Notably, during the early time points of HBV infection, the PF-RC DNA accumulated at significantly higher levels and appeared in a peak followed by a plateau at late time points with dramatically lower levels, implicating the presence of two distinct populations of the PF-RC DNA. Importantly, the PF-RC DNA at earlier peak is entecavir (ETV)-resistant, whereas the PF-RC DNA at posterior days is ETV-sensitive. An interpretation is that the PF-RC DNA at earlier peak represents "input viral DNA" derived from HBV inoculum, whereas the PF-RC DNA at late time points represents the *de novo* product of the viral reverse transcription. The existence of two populations of the PF-RC DNA having a distinct kinetic profile and ETV-sensitivity implicated that intracellular amplification via the viral reverse transcription greatly contributes to the maintenance of cccDNA pool during HBV infection. As such, we concluded that the cccDNA level is stably maintained by continuing replenishment of cccDNA primarily through intracellular amplification in the HepG2-NTCP cell line.

1. Introduction

Hepatitis B virus (HBV) is a viral pathogen that currently infects almost 257 million people worldwide. Hepatitis B related liver cirrhosis and hepatocellular carcinoma resulted in 887000 deaths [WHO 2017]. In chronically HBV infected patients, the risk of developing liver cancer and cirrhosis can significantly increase (El-Serag, 2012; Papatheodoridis et al., 2015; Lee et al., 2017). HBV is a member of the Hepadnaviridae family which are hepatotropic DNA viruses infecting certain mammalian and avian host. HBV surface proteins are composed of three domains: S, preS 2, and preS 1. HBV virions initially attach to hepatocytes via heparan sulfate proteoglycans (HSPGs). Subsequently, pre-S1 envelope protein engages to sodium taurocholate co-transporting polypeptide (NTCP) which has been recently identified as specific receptor for HBV entry (Schulze et al., 2007; Yan et al., 2012). Myrcludex B which is synthetic PreS1 peptide, blocks NTCP mediated HBV entry (Iwamoto et al., 2014; Churin et al., 2015). The synthesis of incoming virion DNA starts with the conversion of a partially double-stranded, relaxed circular DNA (RC DNA) genome into a covalently closed circular DNA (cccDNA), which is an episomal template for viral RNA synthesis (Nassal, 2015). In the cytoplasm, the pregenomic RNA is packaged into subviral core particles along with virus encoded reverse transcriptase (polymerase), and viral pgRNA is then reverse transcribed to the viral DNA inside the capsid by the reverse transcriptase (Nassal, 2008; Seeger and Mason, 2015). Core particles containing the mature viral DNA interact with viral envelope proteins embedded in endoplasmic reticulum (ER), the enveloped particles are released extracellularly via budding process. Alternatively, the core particles may reenter to the nucleus to become cccDNA, via a pathway that is often called intracellular pathway for cccDNA biogenesis (Seeger and Mason, 2015). Previous studies has shown that in HBV DNA replication, RC DNA contributes to establishment of PF-RC DNA and cccDNA either by

* Corresponding author.
** Corresponding author.
E-mail addresses: blseong@yonsei.ac.kr (B.L. Seong), wsryu@yonsei.ac.kr (W.-S. Ryu).

https://doi.org/10.1016/j.antiviral.2019.01.004
Received 5 November 2018; Received in revised form 19 December 2018; Accepted 9 January 2019
Available online 11 January 2019
0166-3542/

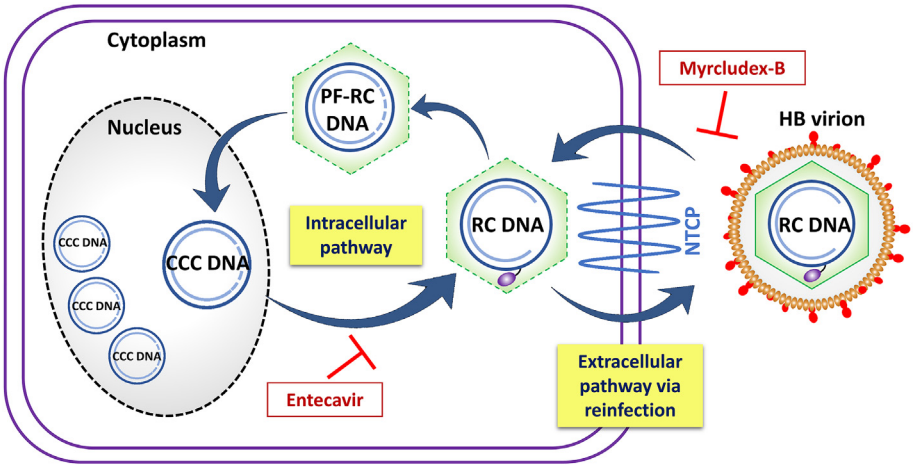

Fig. 1. Schematic illustration of cccDNA amplification pathways in HepG2-NTCP cell line. NTCP mediates HB virus entry. In the cytoplasm, partial un-coating of the capsid protein and plus strand DNA synthesis triggers removal of viral polymerase from the RC DNA which forms PF-RC DNA. Following nuclear import of the PF-RC, cccDNA is established in the nucleus and act as template for transcription of viral RNAs. RC DNA is formed inside nucleocapsids as a result of reverse transcription. Assembled virions may release from the infected cell and re-infect the cells which contributes to the extracellular amplification of cccDNA. Alternatively during intracellular cccDNA amplification pathway, the RC-DNA containing nucleocapsids may convert to cccDNA by nuclear re-import. Myrcludex B as an entry inhibitor, blocks virus entry therefore inhibits extracellular cccDNA amplification pathway. Nucleot(s)ide analogs such as ETV impede intracellular cccDNA amplification by interrupting viral reverse transcription. PF-RC, protein free-relaxed circular; CCC, covalently closed circular; RC, relaxed circular.

"extracellular" and "intracellular" amplification pathways (Guo et al., 2007). Extracellular pathway occur following re-entry of virus particles. Alternatively, intracellular pathway constitutively produce cccDNA by nuclear re-import of RC DNA containing nucleocapsids (Fig. 1).

cccDNA is a hallmark of viral persistence and represents the viral resistance during antiviral therapy (Zoulim, 2005; Nassal, 2015; Li and Urban, 2016). In order to control HBV infection it is imperative to understand the early molecular events involved in cccDNA formation. However the mechanism of cccDNA generation and regulation is not completely understood. Based on viral RC DNA structure described above, it was speculated that during the conversion of RC DNA to cccDNA, the viral polymerase should be removed from 5′ end of minus strand DNA, which is a prerequisite for the ligation of minus strand DNA ends. Studies have shown that removal of the HBV polymerase linked to the viral DNA genome, only occurs after the maturation of plus strand DNA (Guo et al., 2010; Königer et al., 2014). The removal of HBV polymerase from RC DNA, yields a characteristic DNA replication intermediate that is known as protein-free (PF) RC DNA. The PF-RC DNA initially was observed from studies via transfections as well as inducible HBV replication (Gao and Hu, 2007; Guo et al., 2007). HBV PF-RC DNA is more abundant than cccDNA in a HBV replicating cell line or in HepAD38 cells. The PF-RC DNA was reported to be detectable only in the nucleus (Gao and Hu, 2007) while, others showed that the PF-RC DNA is present in both nucleus and cytoplasm (Guo et al. 2007, 2012). However, these studies have been performed in a HBV replicating cell line rather than HBV infection system. This finding needs to be validated by using HBV infection.

To evaluate the HBV protein - free DNA intermediates in our infection model, we studied kinetics of PF-RC as well as cccDNA up to 4 weeks in HBV infected HepG2-NTCP cell line. Our experimental evidence obtained from detailed characterization of HBV DNA species and accumulation kinetics during *de novo* HBV infection of human hepatoma cells is consistent with the hypothesis that protein-free RC DNA is the precursor of cccDNA.

2. Materials and methods

2.1. Cell culture

The human hepatoma cell line HepG2-NTCP cells were cultured in collagen-coated dishes and maintained in DMEM supplemented with 10% FBS and 2 mM L-glutamine (Kim et al., 2016) at 37 °C in a 5% CO2 humidified incubator. HepAD38 cells, HepG2 derivatives that express HBV pgRNA in a tetracycline (Tet)-repressible manner (Ladner et al., 1997) were maintained in 1 μg/ml of Tet until induction. HBV replication was induced by maintaining cells in tetracycline-free medium.

2.2. Extraction of viral DNA

Capsid DNA was isolated from HBV infected HepG2-NTCP cells as previously described (Ko et al., 2014). Briefly, cells were lysed in NP-40 lysis buffer (50 mM Tris-HCl [pH 8.0], 100 mM NaCl, 1 mM EDTA, 1% NP-40). After treatment with 0.02 mg/ml DNaseI (Ambion) and 0.2 mg/ml RNaseA treatment of the supernatant (cytoplasmic lysate), nucleocapsids were precipitated with polyethylene glycol at 4 °C overnight. The next day, HBV core particles were disrupted by sodium dodecyl sulfate (SDS) and viral DNA-protein complexes were digested using proteinase K treatment. Viral DNA was extracted with equal amounts of phenol/chloroform, precipitated with 100% Ethanol in the presence of 3M sodium acetate (pH 5.2) and glycogen. Precipitates were rinsed with 70% ethanol and dissolved in TE (10 mM Tris–HCl, pH 8.0, 1 mM EDTA) buffer.

Hirt extraction method was used for protein free DNA isolation (Hirt, 1967). Cells from one 60 mm dish was lysed in 1 ml of 50 mM Tris–HCl (pH 7.5), 10 mM EDTA, 150 mM NaCl and 1% SDS. After 30 min incubation at room temperature, the lysate was transferred into a 2 ml tube followed by addition of 2.5 M KCl and incubation at 4 °C overnight. The Protein free DNA in the lysate was then extracted twice with phenol: chloroform and once with chloroform. After Isoamyl alcohol precipitation, DNA was dissolved in TE buffer and was treated with Plasmid-Safe ATP-dependent DNase (Epicentre) before detection (Hirt, 1967). Since Detection of cccDNA by Southern blotting can severely be suspicious due to the presence of ssDNA species which have a similar electrophoretic mobility and are often present in excess, purified DNA samples were treated by plasmid safe DNase (PsD) which digests single-stranded (ss) and double-stranded linear (dl) but not circular molecules such as cccDNA (Generation 2010).

2.3. Detection of viral DNA by southern blot analysis

Visualization of HBV DNA was performed as previously described (Kim et al., 2016). Prepared DNA samples were loaded onto 1.3% agarose gel, electrophoresed in TAE buffer and transferred onto Hybond-XL membrane. For the detection of DNA on Southern blots, membranes were probed with [^{32}P] labelled full-length HBV genome. Hybridization was carried out in 10 ml hybridization buffer with 1 h pre-hybridization at 65 °C and overnight hybridization at 65 °C followed by a washing with 0.5 × SSC and 0.1% SDS at 65 °C. The

membrane was exposed to a phosphor imaging plate and detected by Autoradiography (BAS 5000, Fujifilm).

2.4. Virus particle production

For HBV infection, cell culture derived Hepatitis B virions purified from HepAD38 cells supernatant were used. Cells were grown in DMEM–F-12 medium supplemented with 5% fetal calf serum (FCS), 500 g/ml G418, 50 μM hydrocortisone-hemisuccinate, 5 μg/ml insulin, 50 U/ml penicillin, and 50 μg/ml streptomycin. For isolation of viral particles, cells were induced by culturing without Tetracycline for 14 days. Briefly, the viral particles were precipitated from 1 to 2 liters of culture medium by adding PEG 8000 to a final concentration of 5% and incubated shaking at 4 °C overnight. After centrifugation, particles in the pellet were resuspended in 1% of the original volume with PBS/FCS for storage at −80 °C.

2.5. HBV infection

For HBV infection, HepG2-NTCP cells were seeded in plates coated with collagen and infected with HBV at 1000 genome equivalents per cell in the presence of 4% polyethylene glycol (PEG 8000; Sigma). The next day, infected cell were washed with phosphate-buffered saline (PBS) and maintained in the medium containing 2.5% dimethyl sulfoxide (DMSO). The medium was changed every other day and samples were maintained until the preparation day at certain time points.

2.6. Cell fractionation

Separation of cytoplasmic and nuclear fractions was performed based on Sigma celLytic Nuclear extraction kit protocol with minor modification. Cells from 70 to 90% confluent monolayer culture where homogenized with a dounce homogenizer (Bellco) and lysed in a hypotonic buffer containing 100 mM HEPES, 15 mM $MgCl_2$, 100 mM KCL and Nonidet P-40. A portion of the lysate was removed as “whole cell lysate”. Cytoplasmic fraction were separated from nuclei pellet by centrifugation (10,000 × *g* for 30 s at 4 °C). Nuclei pellet was resuspended in extraction buffer (20 mM HEPES, 15 mM $MgCl_2$, 0.42 M NaCl, 0.2 mM EDTA and 25% (v/v) Glycerol including DTT and protease inhibitor cocktail). Samples were mixed and centrifuged 5 min at 10,000 × *g* and nuclear fraction in the supernatant was separated for further experiment.

2.7. Western blot

Western blot analysis was performed as previously described (Kim et al., 2016). Following fractionation, cell lysate was resolved on 12% SDS-polyacrylamide gel and transferred onto Amersham nitrocellulose blotting membrane (GE Healthcare). After blocking step, the membrane was probed with polyclonal rabbit antibody against Calnexin (Santa cruz) and monoclonal rabbit antibody against Histone H3 (Cell signaling). The signal of chemiluminescence reaction visualize by LAS-4000 instrument (Fujifilm).

3. Results

3.1. PF-RC DNA is the first detectable HBV DNA species in HBV infected hepatoma cells

To monitor the viral DNA at early time point following infection, HepG2-NTCP cells were infected. HBV infected cells were prepared by Hirt extraction and HBV DNA intermediates were measured by Southern blot analysis as described in material and methods. First, it was observed that a protein-free RC DNA (PF-RC), become detectable as early as 12 hpi (hours post infection) prior to cccDNA formation, which become detectable substantially at 2 dpi (days post infection) (Fig. 2A). At early time point, the PF-RC DNA was abundant form of HBV protein free DNA detected in HBV infected HepG2-NTCP cells. Southern blot results also showed the PF-RC DNA signal from viral input “inoculum” increased until 3 dpi, along with gradual accumulation of cccDNA (Fig. 2B). The result indicated that the PF-RC DNA was detectable prior to the detection of cccDNA, implicating that the PF-RC DNA might play a role in the upstream events of cccDNA formation.

3.2. Subcellular localization of PF-RC and cccDNA

To gain further insight into the precursor-product relationship between the PF-RC DNA and cccDNA, we looked for subcellular localization of protein-free DNA in cytoplasmic and nuclear fractions at early infection time points that help us to follow conversion process step by step. HBV infected cell samples were harvested for fractionation from 12 hpi up to 3 dpi. Southern blot analysis demonstrated that the PF-RC DNA appears in both cytoplasmic and nuclear fractions of infected HepG2-NTCP cell line. However at 12 hpi, the PF-RC DNA was more accumulated in the cytoplasmic fraction compare to the nuclear fraction (Fig. 3). cccDNA on the other hand was only existed in the nuclear fraction of HBV infected cells and become detectable after 2 dpi (Fig. 3). This suggests that the protein-removal from the input viral DNA did occur in the cytoplasm, perhaps inside the nucleocapsid. This evidence further reinforce the hypothesis that PF-RC DNA may represent a precursor to cccDNA formation.

3.3. Accumulation kinetics of HBV DNA species in HBV infected hepatoma cells

Next, we sought to observe the kinetics of PF-RC and cccDNA for up to 30 days following HBV infection. In addition, capsid-associated DNA was extracted from cytoplasmic capsid. Consistent with the data shown in Fig. 2, Southern blot analysis detected the first PF-RC DNA as early as 1 dpi (the earliest time point for this blot), while cccDNA was significantly detectable at 2–3 dpi band it remained largely unaltered for up to 30 days (Fig. 4A). Kinetic profile revealed that, the PF-RC DNA signal appears in a peak at 3 to 6 dpi followed by a plateau with considerably lower level for up to 30 days (Fig. 4B). On the other hand, cccDNA became detectable at 2 dpi with significantly lower level compared with that of PF-RC DNA at 2 dpi. By contrast to the PF-RC DNA, cccDNA level remained unaltered for up to 30 dpi. Interestingly, following 6 dpi, the cccDNA level became comparable to that of the PF-RC DNA (Fig. 4A and B).

The bimodal kinetic property suggests the existence of two distinct population of PF-RC DNA species in HBV infected cells, where the early strong peak represents the PF-RC DNA species derived from the input “inoculum” HBV virion DNA, while the later lower level plateau most likely represents the PF-RC DNA species produced *de novo* via the viral reverse transcription. Also, the slope of earlier peak implicated that it may take 3–6 days for the complete conversion of the input PF-RC DNA to cccDNA, as the peak reached its maximal level at 2–3 dpi but lower level at 6 dpi. Noteworthy, comparing the initial accumulation of PF-RC DNA (Input DNA at 1 to 3 dpi, average signal intensity 68.6%) to the amount of newly formed cccDNA (from 1 to 3 dpi, average signal intensity 19.9%), it is clear that the conversion of the input PF-RC DNA to cccDNA in HepG2-NTCP cell is inefficient, as only a small fraction (29%) of the input virion DNA is converted to cccDNA (Fig. 4B).

Intracellular capsid-associated DNA which was examined in parallel, revealed the kinetic profile having two peaks with a separation of peaks at 3 dpi (Fig. 4C and D). The first strong signal detected at the first two days after infection is most likely to represent the input viral DNA, while the second peak at 12 dpi most likely represents the DNA products of intracellular amplification through viral reverse transcription. A possibility that the PF-RC DNA strongly detected at 1 dpi represents the “inoculum” virion DNA simply attached to plasma membrane of the cell, and extensive PBS wash at 16 h post infection removed

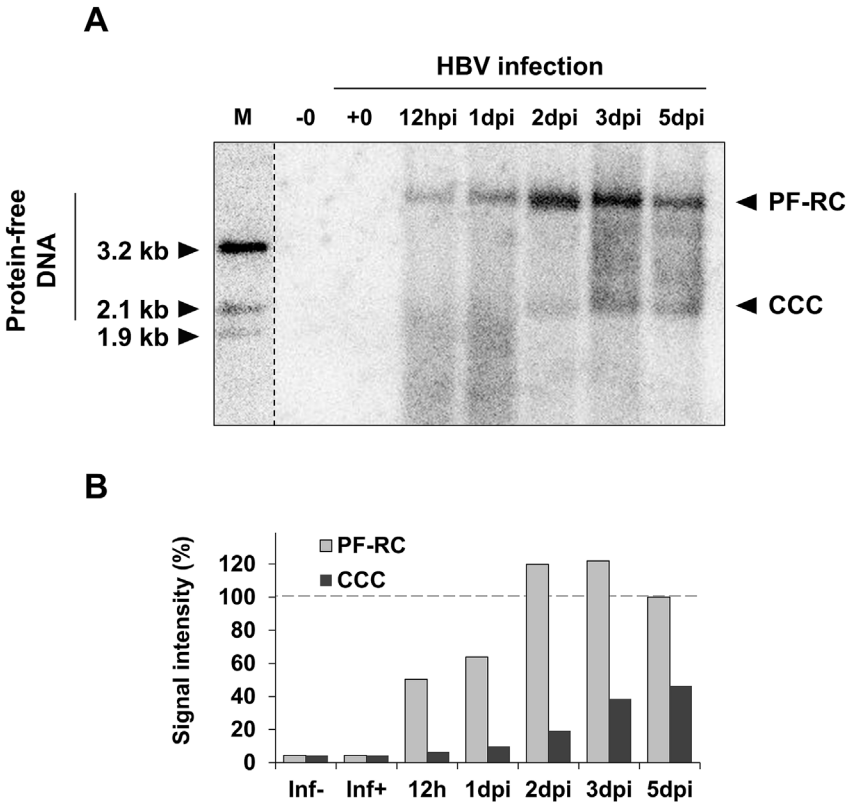

Fig. 2. Detection of PF-RC and cccDNA at early time points following HBV infection in HepG2-NTCP cell line. **(A)** HepG2-NTCP cells were infected with cell culture derived Hepatitis B virus. 1 day after infection, cells were washed and maintained in culture medium containing 2.5% DMSO and were prepared at indicated time points, except for 12 hpi prepared sample which was gathered earlier. Protein free HBV DNA was extracted by Hirt method and was detected by Southern blot. A size marker (3.2, 2.1, 1.9 and 1.4 kb) was co-electrophoresed, indicated by a rightward open arrow. DNA blots were detected using HBV specific radioisotope labelled probe. **(B)** Quantification of the PF-RC and cccDNA signal. PF-RC, protein free-relaxed circular; CCC, covalently closed circular; hpi, hours post infection; dpi, days post infection. The relative intensities of viral PF-RC DNA and cccDNA signals in each sample were considered as percentage of the signals from the PF-RC at 5 dpi (last lane in panel A) and were plotted in a graph shown in panel B. PF-RC, protein free-relaxed circular; CCC, covalently closed circular; M, size marker; hpi, hours post infection, dpi; days post infection.

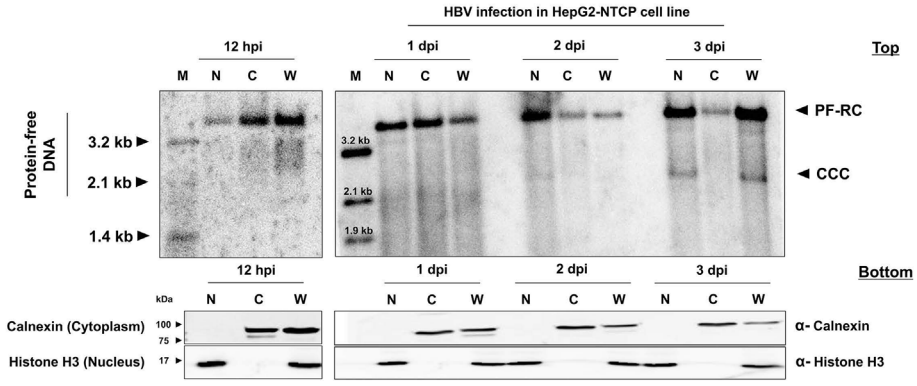

Fig. 3. Subcellular distribution of HBV protein free DNA in HepG2-NTCP cells. **(Top)** HBV infected HepG2-NTCP cells were lysed at 1 dpi, 2 dpi and 3 dpi. Hirt DNA extracted from the lysates of whole cell, cytoplasm, and nuclei of HepG2-NTCP cells and analyzed by Southern blot hybridization. **N**: Nuclear fraction, **C**: Cytoplasmic fraction, **W**: Whole cell lysate. Fractionation procedure is described in material and method section. **(Bottom)** Cell fraction specific markers detected by western blot analysis. Calnexin as cytoplasmic fraction indicator was detected by polyclonal rabbit antibody against Calnexin (Santa cruz). Nuclear fraction was recognized by monoclonal rabbit antibody against Histone H3 (Cell signaling). PF-RC, protein free-relaxed circular; CCC, covalently closed circular; M, size marker; hpi, hours post infection, dpi; days post infection.

all the virus particles that had not been attached to the cellular membrane, leaving high density HBV virions that were tightly attached to the cell membrane or vesicles by help of PEG. Interestingly, the lower DNA level (i.e. eclipse) between two peaks was evident at 3 dpi, suggesting that it may take 3 days for the complete conversion of input virion DNA to cccDNA.

3.4. Intracellular amplification pathway is critical for cccDNA accumulation

The kinetic observation led us to speculate the existence of two distinct PF-RC DNA species, in which the PF-RC DNA present after 6 dpi represents the PF-RC DNA produced via viral reverse transcription. To evaluate this possibility, we examined the PF-RC DNA from 3 dpi to 30 dpi with or without entecavir (ETV) treatment (Fig. 5A). Cells were infected with HBV and were treated with 40 nM ETV in a mixture with cell culture medium every other day starting from 1 dpi. Cells were maintained and prepared for HBV DNA detection from. The graph in Fig. 5 demonstrated that the PF-RC DNA at early stage of the infection course (3–6 dpi) was not affected by drug treatment. The second population of PF-RC DNA (15–30 dpi) however, showed strong sensitivity to ETV treatment in HBV infected HepG2-NTCP cells (Fig. 5A and B). This further confirms the existence of two population of PF-RC DNA where the first population of PF-RC DNA may represent “input viral DNA”, whereas the second PF-RC DNA at later points is the product of the viral reverse transcription. The viral capsid-associated DNA continuously decreased following ETV treatment. More specifically, following 15 dpi, the level of capsid DNA intermediates dramatically decreased, with almost no detectable DNA at 30 days post infection (Fig. 5C).

3.5. The recovery of viral DNA following the drug withdrawal

The observation that not only the PF-RC DNA but also cccDNA level was suppressed by ETV treatment (Fig. 5B) suggests that both the PF-RC DNA and cccDNA are equally regulated by viral reverse transcription. It

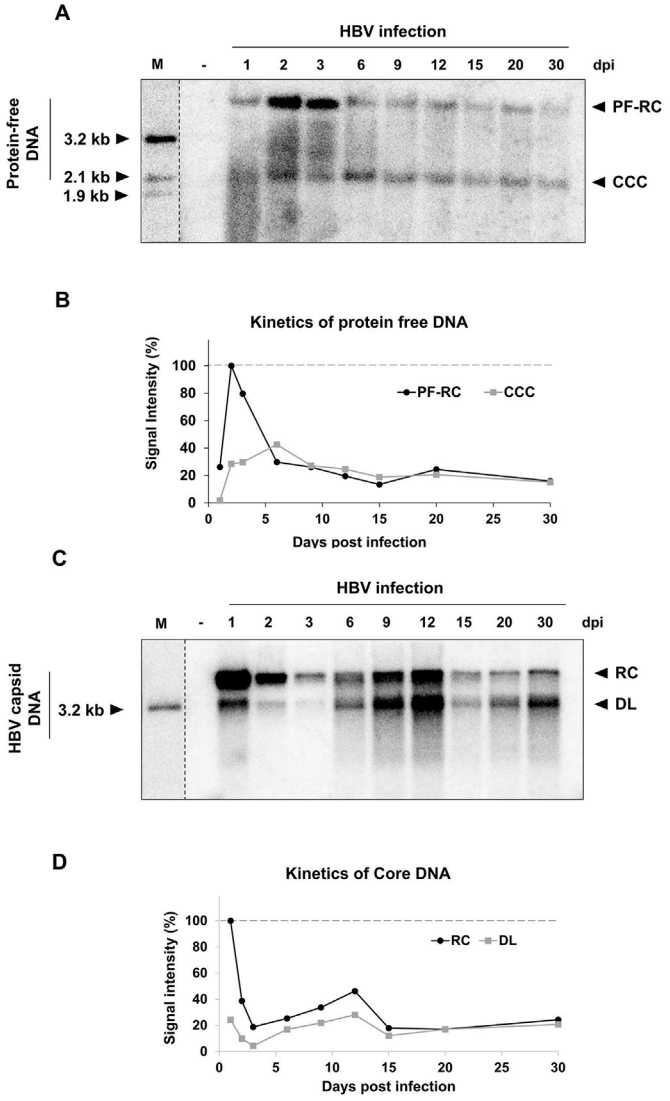

Fig. 4. Kinetics of HBV DNA intermediates during time course infection in HepG2-NTCP cell line. **(A)** The position of a major protein free HBV DNA product derived from HBV infected HepG2- NTCP cells are indicated. First lane (−) is related to negative control in which no virus was inoculated. Upper band shows signal intensity for PF-RC and the bands in the bottom correlates to cccDNA about 2 kb length. Samples were prepared at certain intervals during long term infection starting from 1 day up to 1 month post infection. dpi, days post infection. **(B)** Line graph demonstrating bimodal pattern of PF-RC formation and cccDNA accumulation during extended HBV infection. The levels of viral PF-RC DNA and cccDNA were quantified from the Southern blots shown in panel A, and imposed on the graph. Signal intensity versus time is indicated in Y and X axis respectively. Signals in each sample were considered as percentage of the signals from the PF-RC at 2 dpi (highest level detected in panel A). **(C)** Intracellular HBV core DNA. In a similar copy set of samples, cells were prepared using routine Southern blot technique in order to purify intracellular HBV capsids. Following viral particle precipitation and capsid breakdown, viral DNA was precipitated and cleaned by phenol chloroform isoamyl alcohol 2 times. Purified DNA samples were loaded on agarose gel along with a 3.2 kb size marker. A full length HBV DNA fragment was used to produce radiolabelled probe by extension of random oligonucleotides. RC, relaxed circular; DL, duplex linear; SS, single-stranded DNAs are denoted by the leftward arrowheads. **(D)** Quantification analysis of the virus capsid DNA alternation during 30 days HBV infection. Data represent the means of results from two independent experiments. PF-RC, protein free-relaxed circular; CCC, covalently closed circular; RC, relaxed circular; DL, duplex linear; M, size marker; dpi, days post infection.

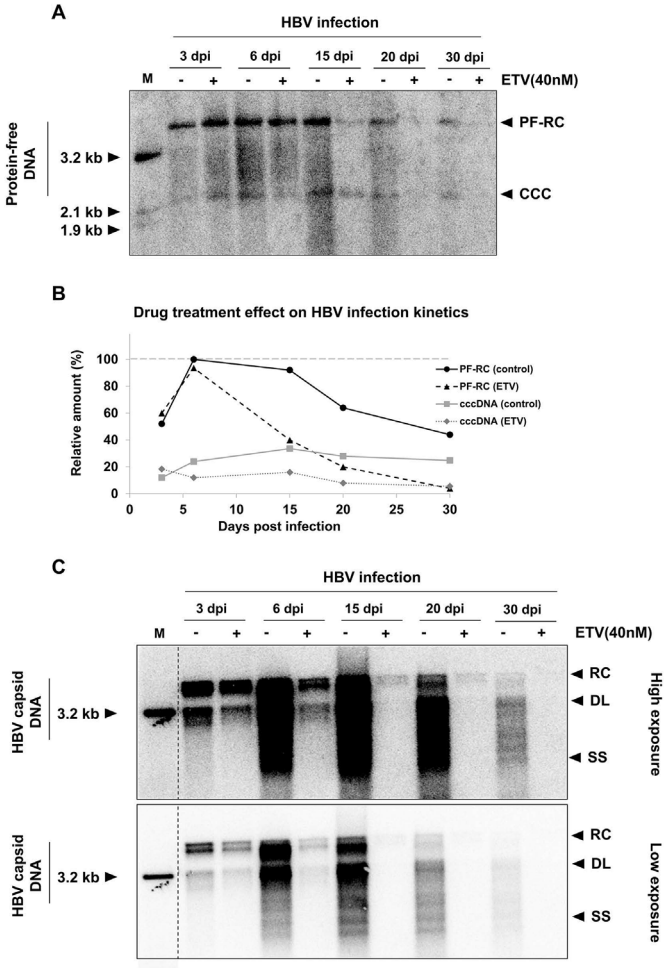

Fig. 5. The effect of ETV treatment on the viral DNA. **(A)** HBV infected HepG2-NTCP cells were treated with 40 nM ETV every other day from starting from first day post infection. Protein free DNA was purified and analyzed by Southern blot. Drug was mixed with the cell culture medium containing 2.5% DMSO. Upper, shows higher exposure during autoradiography versus bottom, which shows less background. **(B)** Quantitative comparison for accumulation of PF-RC and cccDNA in presence (ETV) and absence (Control) of drug in a time period of 30 days. Values from 6 dpi of PF-RC DNA were considered as 100%. **(C)** The effect of ETV treatment on the viral DNA. RC, relaxed circular; DL, duplex linear; SS, single-stranded DNAs. Low exposure (up) versus high exposure (Bottom), indicates amount of viral DNA intermediates inside the nucleocapsids following treatment of 40 nM ETV. ETV, ETV. PF-RC, protein free-relaxed circular; CCC, covalently closed circular; RC, relaxed circular; DL, duplex linear; M, size marker; dpi, days post infection.

is intriguing to see whether cccDNA can be restored by the drug withdrawal. To test this hypothesis, the ETV effect on HBV protein free DNA intermediates was characterized. The strategy was to treat HBV infected cells with ETV up to 10 days post infection and then to withdraw drug from cell culture medium and maintain infected cells until one month. The results revealed that the PF-RC DNA continuously decreased with ETV treatment from 15 dpi and after almost 1 week (day 12 to day 20 post infection) of ETV removal, HBV DNA was recovered (Fig. 6). Particularly, DNA signal recovery was clearly detectable by the end time point at 30 days post infection (Fig. 6). Based on PF-RC DNA and cccDNA recovery after drug removal, we conclude that cccDNA amplification via reverse transcription greatly contributes to cccDNA pool in HepG2-NTCP cell line.

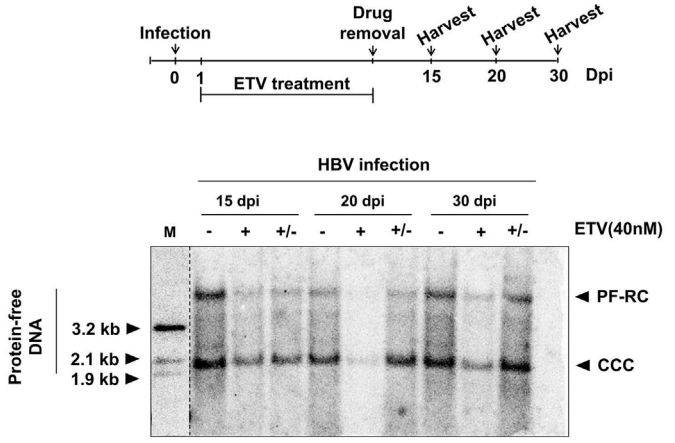

Fig. 6. Recovery of viral DNA following drug withdrawal. HBV infected cells were maintained in the cell culture medium with or without ETV for one month. In one set of samples, drug was added to the cells up to 10 days post infection and was removed from 10 dpi to 30 dpi. Cells were lysed at 15, 20 and 30 time points for DNA analysis. (−); without ETV, (+); with ETV, (±); ETV withdrawal. ETV, ETV; PF-RC, protein free-relaxed circular; CCC, covalently closed circular; M, size marker; dpi, days post infection.

3.6. Contribution of viral re-entry in cccDNA persistence

In addition to intracellular amplification pathway, another route to supplement cccDNA is the viral reentry via NTCP receptor (Fig. 1). To assess the contribution of HBV re-entry to the cccDNA pool in HBV infected HepG2-NTCP cell, we examined the effect of MyrB peptide, an entry inhibitor, by performing HBV infection and treatment of infected cells with MyrB every other day. Treatment of MyrB started from 5 dpi and continued up to a late time point. Five dpi was selected to inhibit re-entry of viral particles, as previous data in Fig. 4 showed that the majority of PF-RC signal from input viral DNA decreased and converted to cccDNA by 6 dpi, and most likely the virion particles produced in one amplification cycle could be secreted and re-entered the cells afterwards. Thus this event possibly could be inhibited by MyrB treatment at 5 dpi. The results indicated the reduction of viral DNA protein free at around 20 dpi or 2 weeks following MyrB treatment. The results showed that MyrB treatment modestly decreased both PF-RC DNA and cccDNA level. (Fig. 7A).

Interestingly, the reduction by MyrB treatment was more pronounced in HBV core DNA intermediates (Fig. 7B). Reduction of HBV DNA following MyrB treatment suggests that the *de novo* infection is occurring in HBV infected HepG2-NTCP cell and viral entry modestly contributes to the maintenance of cccDNA pool.

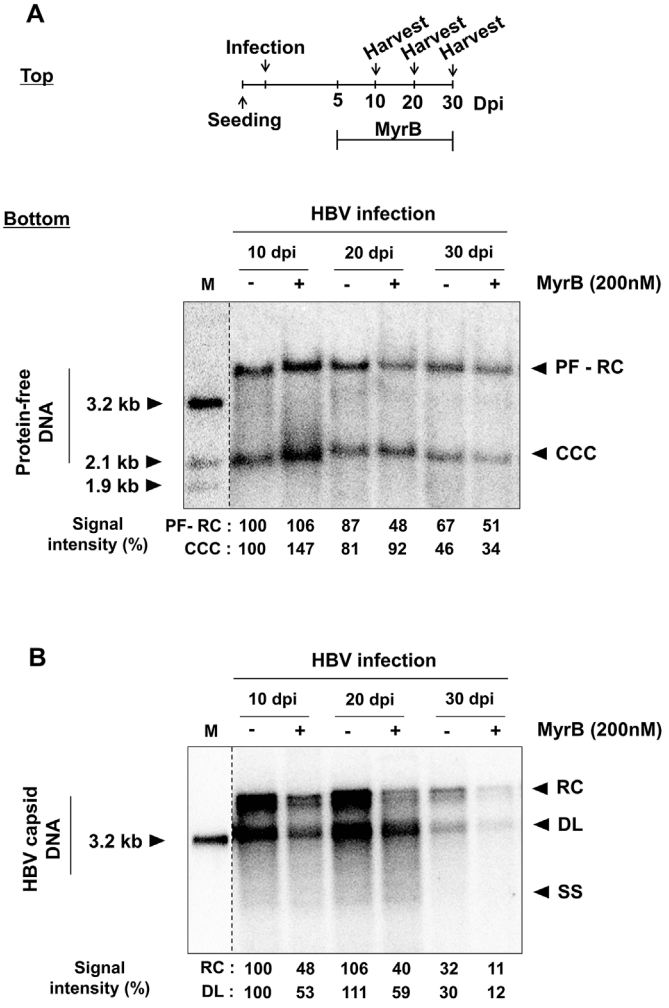

Fig. 7. The effect of Myrcludex B treatment on the viral DNA. (A) Top: HBV infected HepG2-NTCP cells were treated with 200 nM MyrB every other day from starting from five days post infection. **Bottom**: Protein free DNA was purified and analyzed by Southern blot. Drug was mixed with the cell culture medium containing 2.5% DMSO. **(B)** Effect of myrB treatment every other day after 5 days post infection on DNA inside HBV nucleocapsids. Cells were lysed at 7, 10, 15, 20 and 30 dpi. Signal intensities of PF-RC DNA and cccDNA were normalized to the 10 dpi control sample. MyrB, Myrcludex B (PreS1 peptide that competes with virus for receptor attachment); PF-RC, protein free-relaxed circular; CCC, covalently closed circular; M, size marker; dpi, days post infection.

4. Discussion

Although the PF-RC DNA has been described in HBV replicating stable cell line (Guo et al. 2003, 2007; Gao and Hu, 2007; Köck et al., 2010), its precursor-product relationship with cccDNA remain less than clear. In current report, using HepG2-NTCP cell line established previously (Ko et al., 2014), we provided three independent evidence to show that the PF-RC DNA could be a precursor of cccDNA formation in HBV infected cells: (1) kinetic evidence, which showed that the PF-RC DNA appears earlier than cccDNA in HBV infected cell, defining the temporal order of the precursor-product relationship between the PF-RC DNA and cccDNA (Fig. 2), (2) subcellular localization data, which showed that the PF-RC DNA is abundantly detectable first in the cytoplasm and later in the nucleus, where cccDNA is exclusively detectable (Fig. 3), manifesting the logistical feature underlining the precursor-product relationship between the PF-RC DNA and cccDNA, and (3) pharmacological evidence, which showed that unlike to the PF-RC DNA accumulated later (i.e. 6 dpi or later), the PF-RC DNA detected in earlier peak (i.e. 3–6 dpi) is resistant to ETV (Fig. 5). Our interpretation is that the PF-RC DNA in early peak perhaps represent the precursor of cccDNA. Nevertheless, we cannot exclude the formal possibility that PF-RC DNA in the earlier peak might represent a dead-end product of the input DNA derived from inoculum.

In this work, two protein-free viral DNA species were characterized following Hirt extraction of HBV infected cells: the PF-RC DNA and cccDNA. The precursor-product relationship between the PF-RC DNA and cccDNA was supported by three evidence. First, it was confirmed that PF- RC DNA appeared at 12 hpi and cccDNA as its product was mainly accumulated between 1 and 2 dpi (Fig. 2), revealing temporal order between the PF-RC DNA and cccDNA. The notion was further strengthened by the observation that the PF-RC DNA peaked at 2–3 dpi, while cccDNA peaked 6–12 dpi (Figs. 2 and 4). Strong reduction of PF-RC DNA levels between 3 and 6 dpi along with gradual accumulation of cccDNA, implying that the PF-RC DNA converts to cccDNA during a slow process and it remained unaltered afterwards (Fig. 4).

Second, subcellular localization data showed that at 12 hpi, the PF-

RC DNA predominantly accumulated in the cytoplasm (Fig. 3), then it became equally detectable in both cytoplasm and nucleus at 1 dpi, and then finally largely detectable in the nucleus at 2 and 3 dpi. Importantly, exclusive detection of cccDNA in the nucleus is consistent with the precursor-product relationship between PF-RC DNA and cccDNA (Guo et al., 2007). An interpretation is that the removal of the viral polymerase covalently linked to the virion RC DNA (i.e. the PF-RC DNA formation) takes place in the cytoplasm following intracellular uptake of the virion particles. Subsequently, such formed PF-RC DNA migrates to the cell nucleus where it is converted to cccDNA.

Third, the ETV treatment clearly revealed the presence of two different PF-RC DNA species that are distinct with respect to the response to the drug treatment. The presence of two pharmacological distinct PF-RC DNA species enable us to gain insight into the origin of the two PF-RC DNA species. We speculated that the PF-RC DNA in earlier peak (e.g. 3–6 dpi), which is ETV-resistant, is derived from the "inoculum", while the PF-RC DNA in later-plateau (e.g. 15 dpi or later), which is ETV-sensitive, is *de novo* synthesized product of viral reverse transcription following the cccDNA formation (Fig. 5B). In addition, inhibiting *de novo* infection via extracellular particles using MyrB treatment (Fig. 7) indicated the importance of extracellular cccDNA dynamics.

We considered that our HepG2-NTCP cell line is robust in at least two respects: (i) HBV infection efficiency is rather higher, approaching 60% at 1000 moi, as previously reported (Ko et al., 2015), and (ii) the cccDNA is measurably detectable by Southern blot analysis, while many others have to employ PCR for the detection of cccDNA. Nonetheless, our HepG2-NTCP cell system has some limitations. First, it was noted that only a small fraction (~29%) of the input virion DNA is converted to cccDNA (Fig. 4B), as evidenced by much abundant detection of the PF- RC DNA compared to the cccDNA. In other words, the conversion of the PF-RC DNA to cccDNA is slow (i.e. a plateau at 3 dpi) and appears a rate limiting process in our HepG2-NTCP cell. Possibly the inefficiency for the cccDNA conversion, could be attributable to the restriction imposed by host. It is plausible that the inefficiency of cccDNA conversion appears to be inherent features of HBV infection, as only a few copy of cccDNA per cell is sufficient for the establishment of persistent infection. Second, the experimental variability in kinetic behavior of the HBV DNA species between experiments was inevitable in our hand. It was noted that the experimental variability stems from either cell death at later time points or excessive cell proliferation during long-term culture. The work is in progress to find out cell culture conditions that give rise to more reproducible outcomes. Noteworthy however, the amount of cccDNA detected here is much more abundant than other more physiological infection models such as HepaRG and primary human hepatocytes in literature (Gao and Hu, 2007; Köck et al., 2010; Cui et al., 2015a). It is tempting to consider that our HepG2-NTCP cell might provide opportunity for elucidation of the host factors involved in the cccDNA conversion.

Importantly, current study provided clear evidence for the existence of two distinct routes that contribute to the accumulation of cccDNA (Figs. 4 and 5). First, in early in HBV infection, cccDNA is exclusively derived from the virion RC DNA via viral entry, termed "extracellular pathway". Once, HBV infection has been established following cccDNA formation, the cccDNA is replenished by the second pathway involving the viral reverse transcription; this is termed "intracellular pathway". It is notable that, the two pathways are distinct in a few respect. First, their contribution to the cccDNA accumulation is temporally distinctive (Fig. 1); the former contributes to the early establishment of HBV infection, while the latter contributes to the maintenance of persistent HBV infection (Fig. 4). Second, two pathways are distinct in pharmacologic aspect: the former is ETV-resistant, whereas the latter is ETV-sensitive (Fig. 5A and B) (Gao and Hu, 2007; Guo et al., 2007; Levrero et al., 2009; Guo and Guo, 2015). Third, they are distinct with respect to its association with endocytosis: the former is associated with endocytic pathway, where the latter is not (Fig. 1).

The cccDNA represents a hallmark of not only viral persistence during chronic HBV infection but also drug resistance during the antiviral therapy (Zoulim, 2004; Colonno et al., 2006; Locarnini and Mason, 2006; Tenney et al., 2007; Villet et al., 2007; Baldick et al., 2008). It is thus valuable to identify host factors involving in the conversion of the PF-RC DNA to cccDNA in order to find novel approach to eliminate cccDNA persistence. Recently, several host factors that are essential for cccDNA conversion in experimental system have been reported, including tyrosyl DNA phosphodiesterase-2 (Tdp2) (Cui et al., 2015b), flap structure-specific endonuclease 1 (FEN1) (Kitamura et al., 2018) and DNA polymerase κ (POLK) (Qi et al., 2016). However, the exact contribution of these host factors for cccDNA formation needs to be validated in HBV infected cells. Besides to those host factors, in order to fulfill the biochemical steps involved in the cccDNA formation, additional host factors need to be discovered.

Overall, through robust HBV infection in the HepG2-NTCP cell, data presented here, suggested that the PF-RC DNA, which appears early in infection and is abundantly detectable in the cytoplasm, exhibits ETV-resistance and migrates to the nucleus, could serve as the precursor of cccDNA formation in the nucleus. Further corresponding studies are required to unveil exact mechanisms involved in the process of cccDNA formation.

It is hoped that the identification of the PF-RC DNA as a precursor of cccDNA can lead to delineation of biochemical steps involved in the cccDNA formation and uncover host factors involved in the cccDNA formation. While this article was in preparation, Ko et al., (2018) described sluggish kinetics of HBV in the same infection model defining moderate growths in cccDNA levels during extended infection course in culture system. Mentioned study and our work examined the hypothesis of PF-RC and cccDNA precursor product relationship in the actual infection system as compared to well-studied transfection system.

Acknowledgments

We wish to thank Dr. Chunkyu Ko for his technical advice at early stages of this project. HepAD38 cells were kindly provided by Dr. Christoph Seeger at Fox Chase Cancer Center. Myrcludex B was a generous gift from Stephan Urban (University Hospital Heidelberg, Heidelberg, Germany). This work was supported by National Research Foundation of Korea (NRF) grant NRF-2015R1A2A2A01005938 funded by the South Korean government.

Appendix A. Supplementary data

Supplementary data to this article can be found online at https://doi.org/10.1016/j.antiviral.2019.01.004.

References

Baldick, C.J., Tenney, D.J., Mazzucco, C.E., Eggers, B.J., Rose, R.E., Pokornowski, K.A., Yu, C.F., Colonno, R.J., 2008. Comprehensive evaluation of hepatitis B virus reverse transcriptase substitutions associated with entecavir resistance. Hepatology 47 (5), 1473–1482.

Churin, Y., Roderfeld, M., Roeb, E., 2015. Hepatitis B virus large surface protein: function and fame. Hepatobiliary Surg. Nutr. 4 (1), 1.

Colonno, R.J., Rose, R., Baldick, C.J., Levine, S., Pokornowski, K., Yu, C.F., Walsh, A., Fang, J., Hsu, M., Mazzucco, C., 2006. Entecavir resistance is rare in nucleoside naive patients with hepatitis B. Hepatology 44 (6), 1656–1665.

Cui, X., Guo, J.-T., Hu, J., 2015a. Hepatitis B virus covalently closed circular DNA formation in immortalized mouse hepatocytes associated with nucleocapsid destabilization. J. Virol. 89, 9021–9028.

Cui, X., McAllister, R., Boregowda, R., Sohn, J.A., Ledesma, F.C., Caldecott, K.W., Seeger, C., Hu, J., 2015b. Does tyrosyl DNA phosphodiesterase-2 play a role in hepatitis B virus genome repair? PLoS One 10 (6), e0128401.

El-Serag, H.B., 2012. Epidemiology of viral hepatitis and hepatocellular carcinoma. Gastroenterology 142 (6), 1264–1273 e1261.

Gao, W., Hu, J., 2007. Formation of hepatitis B virus covalently closed circular DNA: removal of genome-linked protein. J. Virol. 81 (12), 6164–6174.

Guo, H., Jiang, D., Zhou, T., Cuconati, A., Block, T.M., Guo, J.-T., 2007. Characterization of the intracellular deproteinized relaxed circular DNA of hepatitis B virus: an intermediate of covalently closed circular DNA formation. J. Virol. 81 (22), 12472–12484.

Guo, H., Mao, R., Block, T.M., Guo, J.-T., 2010. Production and function of the cytoplasmic deproteinized relaxed circular DNA of hepadnaviruses. J. Virol. 84 (1), 387–396.
Guo, H., Xu, C., Zhou, T., Block, T.M., Guo, J.-T., 2012. Characterization of the host factors required for hepadnavirus covalently closed circular (ccc) DNA formation. PLoS One 7 (8), e43270.
Guo, J.-T., Guo, H., 2015. Metabolism and function of hepatitis B virus cccDNA: implications for the development of cccDNA-targeting antiviral therapeutics. Antivir. Res. 122, 91–100.
Guo, J.-T., Pryce, M., Wang, X., Barrasa, M.I., Hu, J., Seeger, C., 2003. Conditional replication of duck hepatitis B virus in hepatoma cells. J. Virol. 77 (3), 1885–1893.
Hirt, B., 1967. Selective extraction of polyoma DNA from infected mouse cell cultures. J. Mol. Biol. 26 (2), 365–369.
Iwamoto, M., Watashi, K., Tsukuda, S., Aly, H.H., Fukasawa, M., Fujimoto, A., Suzuki, R., Aizaki, H., Ito, T., Koiwai, O., 2014. Evaluation and identification of hepatitis B virus entry inhibitors using HepG2 cells overexpressing a membrane transporter NTCP. Biochem. Biophys. Res. Commun. 443 (3), 808–813.
Kim, W., Lee, S., Son, Y., Ko, C., Ryu, W.-S., 2016. DDB1 stimulates the viral transcription of hepatitis B virus via HBx-independent mechanisms. J. Virol. 90 (21), 9644–9653.
Kitamura, K., Que, L., Shimadu, M., Koura, M., Ishihara, Y., Wakae, K., Nakamura, T., Watashi, K., Wakita, T., Muramatsu, M., 2018. Flap endonuclease 1 is involved in cccDNA formation in the hepatitis B virus. PLoS Pathog. 14 (6), e1007124.
Ko, C., Chakraborty, A., Chou, W.-M., Hasreiter, J., Wettengel, J.M., Stadler, D., Bester, R., Asen, T., Zhang, K., Wisskirchen, K., 2018. Hepatitis B virus genome recycling and de novo secondary infection events maintain stable cccDNA levels. J. Hepatol. 69 (6), 1231–1241.
Ko, C., Lee, S., Windisch, M.P., Ryu, W.-S., 2014. DDX3 DEAD-box RNA helicase is a host factor that restricts hepatitis B virus replication at the transcriptional level. J. Virol. 88 (23), 13689–13698.
Ko, C., Park, W.-J., Park, S., Kim, S., Windisch, M.P., Ryu, W.-S., 2015. The FDA approved drug irbesartan inhibits HBV-infection in HepG2 cells stably expressing sodium taurocholate co-transporting polypeptide. Antivir. Ther. 20 (8), 835–842.
Köck, J., Rösler, C., Zhang, J.-J., Blum, H.E., Nassal, M., Thoma, C., 2010. Generation of covalently closed circular DNA of hepatitis B viruses via intracellular recycling is regulated in a virus specific manner. PLoS Pathog. 6 (9), e1001082.
Königer, C., Wingert, I., Marsmann, M., Rösler, C., Beck, J., Nassal, M., 2014. Involvement of the host DNA-repair enzyme TDP2 in formation of the covalently closed circular DNA persistence reservoir of hepatitis B viruses. Proc. Natl. Acad. Sci. 111 (40), E4244–E4253.
Ladner, S.K., Otto, M.J., Barker, C.S., Zaifert, K., Wang, G.-H., Guo, J.-T., Seeger, C., King, R.W., 1997. Inducible expression of human hepatitis B virus (HBV) in stably transfected hepatoblastoma cells: a novel system for screening potential inhibitors of HBV replication. Antimicrob. Agents Chemother. 41 (8), 1715–1720.
Lee, H.W., Park, H.J., Jin, B., Dezhbord, M., Han, K.-H., Ryu, W.-S., Kim, S., Ahn, S.H., 2017. Effect of S267F variant of NTCP on the patients with chronic hepatitis B. Sci. Rep. 7 (1), 17634.
Levrero, M., Pollicino, T., Petersen, J., Belloni, L., Raimondo, G., Dandri, M., 2009. Control of cccDNA function in hepatitis B virus infection. J. Hepatol. 51 (3), 581–592.
Li, W., Urban, S., 2016. Entry of hepatitis B and hepatitis D virus into hepatocytes: basic insights and clinical implications. J. Hepatol. 64 (1), S32–S40.
Locarnini, S., Mason, W.S., 2006. Cellular and virological mechanisms of HBV drug resistance. J. Hepatol. 44 (2), 422–431.
Nassal, M., 2008. Hepatitis B viruses: reverse transcription a different way. Virus Res. 134 (1–2), 235–249.
Nassal, M., 2015. HBV cccDNA: viral persistence reservoir and key obstacle for a cure of chronic hepatitis B. Gut 64 (12), 1972–1984.
Papatheodoridis, G.V., Chan, H.L.-Y., Hansen, B.E., Janssen, H.L., Lampertico, P., 2015. Risk of hepatocellular carcinoma in chronic hepatitis B: assessment and modification with current antiviral therapy. J. Hepatol. 62 (4), 956–967.
Qi, Y., Gao, Z., Xu, G., Peng, B., Liu, C., Yan, H., Yao, Q., Sun, G., Liu, Y., Tang, D., 2016. DNA polymerase κ is a key cellular factor for the formation of covalently closed circular DNA of hepatitis B virus. PLoS Pathog. 12 (10), e1005893.
Schulze, A., Gripon, P., Urban, S., 2007. Hepatitis B virus infection initiates with a large surface protein–dependent binding to heparan sulfate proteoglycans. Hepatology 46 (6), 1759–1768.
Seeger, C., Mason, W.S., 2015. Molecular biology of hepatitis B virus infection. Virology 479, 672–686.
Tenney, D.J., Rose, R.E., Baldick, C.J., Levine, S.M., Pokornowski, K.A., Walsh, A.W., Fang, J., Yu, C.-F., Zhang, S., Mazzucco, C.E., 2007. Two-year assessment of entecavir resistance in Lamivudine-refractory hepatitis B virus patients reveals different clinical outcomes depending on the resistance substitutions present. Antimicrob. Agents Chemother. 51 (3), 902–911.
Villet, S., Ollivet, A., Pichoud, C., Barraud, L., Villeneuve, J.-P., Trépo, C., Zoulim, F., 2007. Stepwise process for the development of entecavir resistance in a chronic hepatitis B virus infected patient. J. Hepatol. 46 (3), 531–538.
Yan, H., Zhong, G., Xu, G., He, W., Jing, Z., Gao, Z., Huang, Y., Qi, Y., Peng, B., Wang, H., 2012. Sodium taurocholate cotransporting polypeptide is a functional receptor for human hepatitis B and D virus. elife 1, e00049.
Zoulim, F., 2004. Mechanism of viral persistence and resistance to nucleoside and nucleotide analogs in chronic hepatitis B virus infection. Antivir. Res. 64 (1), 1–15.
Zoulim, F., 2005. New insight on hepatitis B virus persistence from the study of intrahepatic viral cccDNA. J. Hepatol. 42 (3), 302–308.